SCIENTIFIC REPORTS

OPEN

SUBJECT AREAS:
ELECTRONIC MATERIALS AND DEVICES
ELECTROCHEMISTRY
APPLIED PHYSICS
SURFACE CHEMISTRY

Received
5 December 2011

Accepted
4 January 2012

Published
3 February 2012

Correspondence and requests for materials should be addressed to G.S. (gshi@tsinghua.edu.cn)

Ultrahigh-rate supercapacitors based on eletrochemically reduced graphene oxide for ac line-filtering

Kaixuan Sheng, Yiqing Sun, Chun Li, Wenjing Yuan & Gaoquan Shi

Department of Chemistry, Tsinghua University, Beijing 100084, People's Republic of China.

The recent boom in multifunction portable electronic equipments requires the development of compact and miniaturized electronic circuits with high efficiencies, low costs and long lasting time. For the operation of most line-powered electronics, alternating current (ac) line-filters are used to attenuate the leftover ac ripples on direct current (dc) voltage busses. Today, aluminum electrolytic capacitors (AECs) are widely applied for this purpose. However, they are usually the largest components in electronic circuits. Replacing AECs by more compact capacitors will have an immense impact on future electronic devices. Here, we report a double-layer capacitor based on three-dimensional (3D) interpenetrating graphene electrodes fabricated by electrochemical reduction of graphene oxide (ErGO-DLC). At 120-hertz, the ErGO-DLC exhibited a phase angle of −84 degrees, a specific capacitance of 283 microfaradays per centimeter square and a resistor-capacitor (RC) time constant of 1.35 milliseconds, making it capable of replacing AECs for the application of 120-hertz filtering.

Electric double-layer capacitors (DLCs), also called supercapacitors or ultracapacitors, store charges through reversible ion adsorption at electrolyte-electrode interfaces upon applying a voltage[1–4]. This energy-storage mechanism offers DLCs with several desirable properties such as a long cycling life (>10,000 cycles) and high specific power density[5]. Additionally, the specific energy densities of DLCs are several orders of magnitude higher than those of conventional AECs[6]. Therefore, DLCs are promising replacements of AECs for ac line-filtering, leading to reduce the sizes of electronic circuits. However, the poor frequency responses of commercial DLCs are a critical obstacle for this application.

For ac line-filtering, capacitors need to respond harmonically at 120 Hz, the double value of ac frequency (60 Hz, the United States standard) to smooth the leftover ac ripples in power supplies. However, typical DLCs are incapable for ac line-filtering at this frequency. Upon driven by 120-Hz ac, they behave like transmission lines, acting as resistors rather than capacitors[7]. This is mainly due to that the unsuitable pore structures of their electrodes impede high-rate ion diffusions or their high resistances restrict efficient charge transfer[8,9]. Thus, the design and fabrication of highly conductive electrodes with optimized micro-/nano-architectures for facile electron/ion transportations can improve the performances of DLCs in ac line-filtering[10,11].

A variety of materials including onion-like carbon[2], carbon nanotubes (CNTs)[12,13], nickel network[14], carbide-derived carbon[15], polymers[16], and metal oxides[17] have already been explored to fabricate the electrodes of DLCs for improving their rate-capability. However, their performances are still unsatisfactory for ac line-filtering. Recently, a great advancement has been achieved by using graphene to replace conventional carbon materials because of its superior electrical conductivity and high specific surface area[18–21]. However, graphene sheets in these electrodes are still in a stacked geometry and randomly oriented with respect to their current collectors. As a result, the pores in the electrodes are partially inaccessible to the electrolyte[22]. An exception was reported by Miller and co-workers[7]. A DLC based on vertically oriented graphene sheets prepared by chemical vapor deposition (CVD) demonstrated efficient filtering of 120 Hz ac with a RC time constant of about 200 μs. Unfortunately, the CVD method suffers from high cost and complicate procedures, which would strongly limit its commercial applications. Here, we report a DLC with electrodes fabricated by one-step electrochemical reduction of graphene oxide (GO) from its aqueous suspension (ErGO-DLC). The electrodes of ErGO-DLC have a 3D interpenetrating graphene microstructure, which provides the DLC with an ultrahigh-rate capability and high specific capacitance. It is capable of replacing AEC for ac line-filtering. Moreover, the technique reported here is fast, cheap, convenient, environmentally friendly and readily scalable to industrial levels.

Results

The typical electrode of electrochemically reduced graphene oxide (ErGO electrode, Figure 1a) can be prepared by electrolyzing 3 mg ml^{-1} GO aqueous suspension containing 0.1 M lithium perchlorate ($LiClO_4$) on a metal electrode (e.g. Au) at an applied potential of −1.2 V for 10 s (see Supplementary Materials and Methods). During this process, GO sheets were reduced into conductive graphene as reported in the literature[23]. The efficient removal of the oxygenated groups of GO upon electrochemical reduction was also confirmed by Raman and X-photoelectron spectral examinations (Supplementary Fig. S1). The resulting ErGO sheets are more hydrophobic and have weaker electrostatic repulsion and stronger π-π stacking interaction than those of their GO precursors. Thus, they were self-assembled to form 3D interpenetrating networks and deposited onto the substrate electrode upon the driving of electric field[24]. The as-prepared ErGO electrode consists of two parts: a basal layer of approximately 200 nm thick and a porous 3D interpenetrating layer with a thickness of about 20 μm (Figure 1b and 1c, Supplementary Fig. S2). The pore sizes of the network are in the range of several micrometers to larger than ten micrometers, and the pore walls are nearly vertical to the surface of current collector (Figure 1d). Therefore, the micropores in the electrode are fully exposed to the electrolyte for the access of ions to form electrochemical double-layers.

Discussion

To test the performance of ErGO-DLCs, symmetrical cells with a two-electrode configuration were constructed to simulate actual device behavior[25]. Two identical ErGO electrodes shown in Figure 1a were used as the electrodes, and they do not have any binders or conducting additives. It should be noted here that the graphene material of the ErGO electrode is too light to be weighted accurately. Thus, the specific capacitance (C_s) of ErGO-DLC was evaluated in area units (μF cm^{-2})[26–27]. Impedance phase angles of ErGO-DLC at different frequencies are plotted in Figure 2a. The closer the phase angle approaches −90°, the device behaves more like a capacitor. At the phase angle of −45°, the resistance and reactance of the capacitor have equal magnitudes, so the frequency at this point is convenient for comparison. The impedance phase angle of ErGO-DLC reached −45° at 4.2 KHz, and this frequency is much higher than that of an activated carbon DLC (0.05 Hz)[27] or a CNTs DLC (636 Hz)[13]. The phase angle at 120 Hz can be used as a "factor of merit" to measure ac line-filtering performance. At 120 Hz, the impedance phase angle of ErGO-DLC is as large as −84°. This angle is comparable to that of a commercial AEC (−85.5°, Supplementary Fig. S3) and larger than those of any reported DLCs including those based on CVD grown graphene nanosheets (−82°)[7], CNTs (−75°)[13], and activated carbon (0°)[28].

The Nyquist plot of ErGO-DLC is nearly a vertical line (Figure 2b), reflecting its high conductivity and rate capability. The plot does not have a semicircle at high frequencies, implying the fast ion diffusion in the ErGO electrode. A line that intersects the real axis at around −45° was also not observed, suggesting the absence of porous electrode behavior[7]. The equivalent series resistance (ESR) value of the ErGO-DLC is about 0.1 Ω. This value is smaller than that of the DLCs based on graphene films (0.15 Ω)[21] or graphene hydrogels (0.5 Ω)[29] reported previously. The extraordinary low ESR of the ErGO electrode can be attributed to two critical factors: (1) ErGO sheets formed a highly conductive network directly coated on the current collector, providing the electrode with low internal and interfacial resistances; (2) the interconnected micropores of ErGO electrode are fully accessible for ion adsorption/desorption.

Considering the Nyquist plot has a vertical line characteristic of capacitive behavior at low frequencies, a series-RC circuit model was used to stimulate the capacitive and resistive elements of the capacitor. In this model, resistance is the real part of impedance spectrum, and the capacitance (C) was calculated by using the equation of $C = -1/(2\pi fZ'')$, where f is frequency in Hz and Z″ is the imaginary part of the impedance spectrum[9]. C_s is defined as C/S (where C is capacitance and S is the apparent surface area of the electrode; here, S = 1.4 cm^2). The C_s of the capacitor increases from 240 to 325 μF cm^{-2} as the frequency decreases from 10^4 to 1 Hz (Figure 2c). The divergent behavior near 21 kHz is an artifact of the model (where Z″ passes through zero). At 120 Hz, the capacitance of the capacitor was calculated to be 397 μF, and its resistance was measured to be 3.4 Ω, yielding an RC time constant of 1.35 ms. Such a short RC time constant indicates that the ErGO-DLC can be used for 120-Hz filtering (8.3 ms period). In addition, a C_s value of 283 μF cm^{-2} was obtained at 120 Hz, and this value is about 3.2 times that of the DLC based on vertically oriented CVD graphene nanosheets (87.5 μF cm^{-2})[7]. In comparison, the C_s of the capacitor with bare gold electrodes was tested to be less than 11 μF cm^{-2} at 120 Hz (Supplementary Fig. S4). Thus, it is reasonable to conclude that the C_s of ErGO-DLC is mainly attributed to the ion intercalation into the 3D interpenetrating microstructures of ErGO electrodes.

The fast ion diffusion in ErGO-DLC was further confirmed by its extremely small relaxation time constant (τ_0) (Figure 2d). τ_0 is the minimum time needed to discharge all the energy from the device with an efficiency of greater than 50% of its maximum value, and it can be derived from the frequency at maximum C″ [30]. The τ_0 of

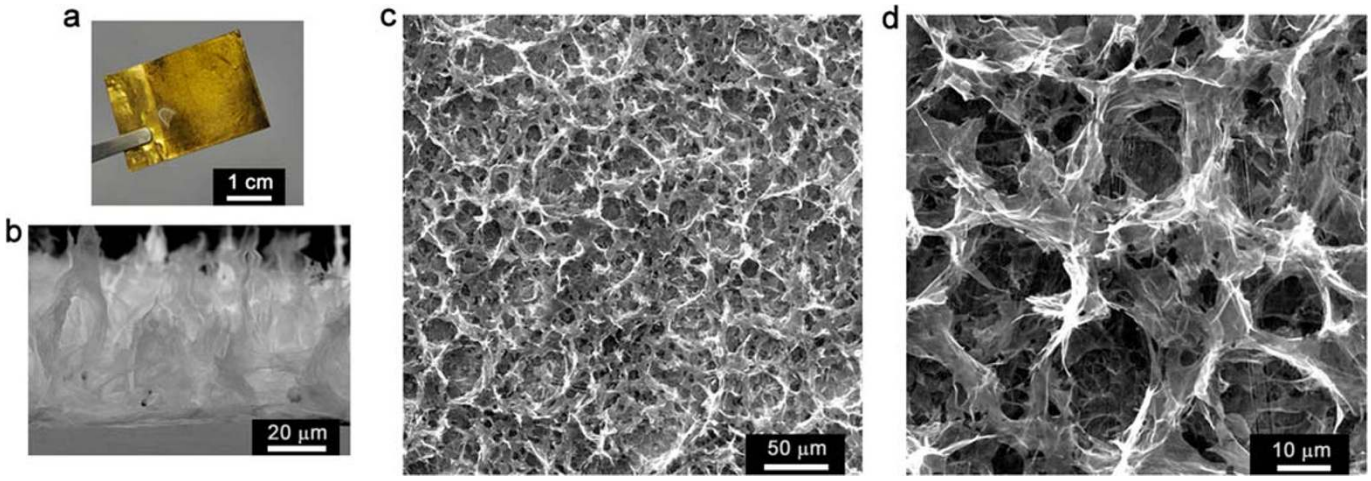

Figure 1 | Microstructure of ErGO electrode. (a) Photograph of an ErGO electrode. (b) Cross-sectional scanning electron microscope image of ErGO electrode. (c, d) Top-view scanning electron microscope images of ErGO electrode with low (c) and high (d) magnifications.

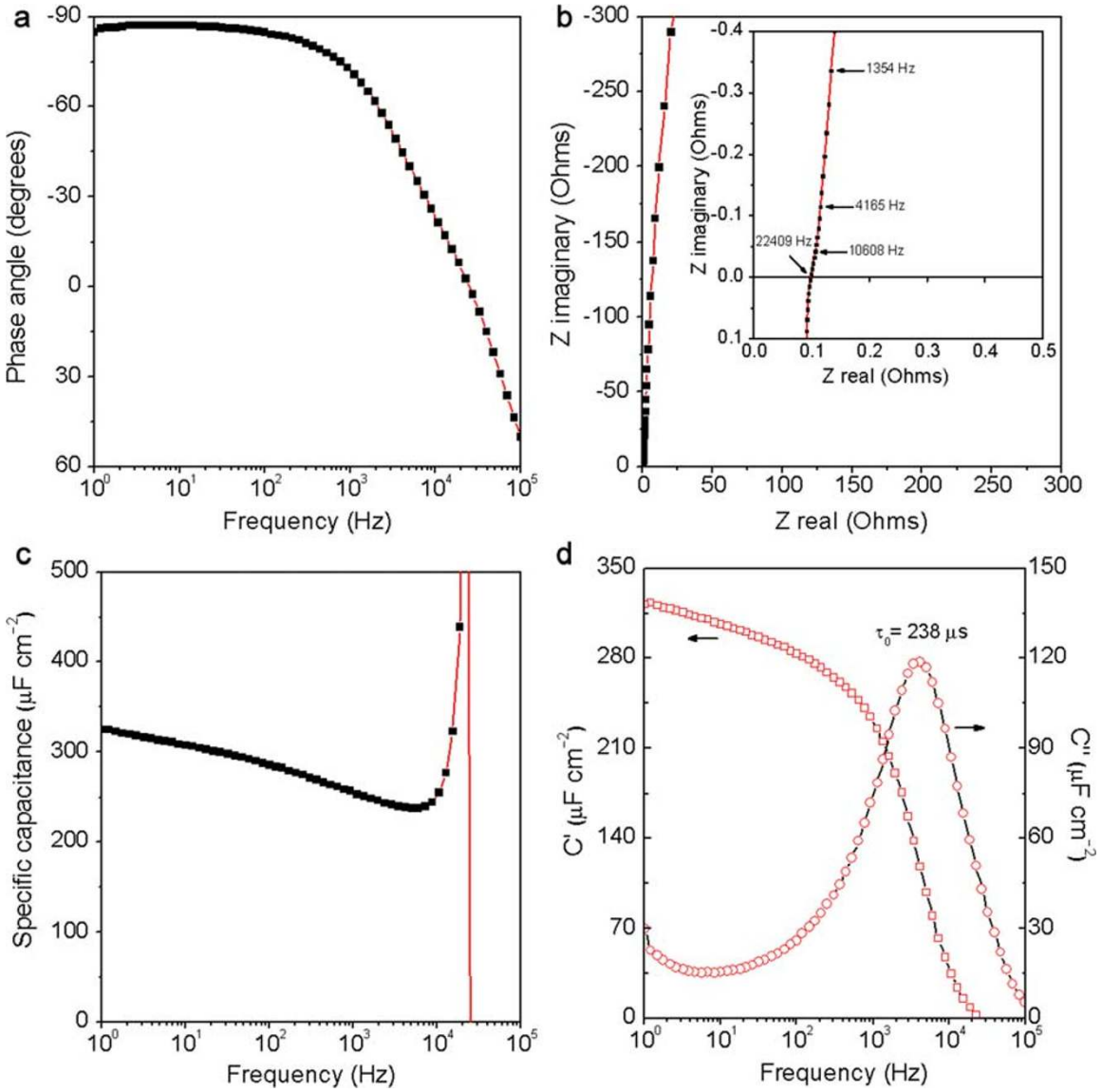

Figure 2 | AC Impedance characterizations of ErGO-DLC. (a) Plot of impedance phase angle versus frequency. (b) Complex plane plot of the impedance; inset: an expanded view in the region of high frequencies. (c) Plot of specific capacitance versus frequency using a series-RC circuit model. (d) Plot of the real or imaginary part (C′ or C″) of specific capacitance versus frequency.

ErGO-DLC was calculated to be 238 μs (4.2 KHz), which is much shorter than those of high-rate DLCs based on CNTs (1.5 ms)[13], onion-like carbon (26 ms)[2], activated carbon (700 ms)[2] and multi-layered graphene film (13.3 ms)[19].

The electrochemical performance of ErGO-DLC was also analyzed using cyclic voltammetry (CV) (Figure 3a). The CV curves of ErGO-DLC keep rectangular in shape at an ultrafast scan rate of 100 V s^{-1}, confirming the formation of an efficient EDLs and fast charge propagations within the electrodes. Even at a scan rate of 400 V s^{-1}, the CV curve remains quasi-rectangular with only a little variance. The discharge current densities exhibit a linear relationship with scan rates in the range of 1–350 V s^{-1} (Figure 3b). To our knowledge, this up-limit of scan rate (e.g. 350 V s^{-1}) for the linear relationship is the highest among any reported capacitors; it is over two orders of magnitude higher than those of typical DLCs and three times higher than that of an onion-like carbon DLC[2].

The discharge curves of ErGO-DLC carried out at the current densities in the range of 40 to 700 μA cm^{-2} are straight lines (Figure 4a), demonstrating an ideal double layer capacitor behavior. Furthermore, no voltage drop was observed at the beginning of discharge (IR drop), suggesting an extraordinary low ESR of ErGO-DLC. This result correlates well with the ac impedance measurements (Figure 2b and 2d). The C_s of the capacitor was calculated to be 487, 480, 462 or 457 μF cm^{-2} according to the discharge curve recorded at a current density of 40, 80, 400 or 700 μA cm^{-2}. When the discharge current density was further increased to 800 μA cm^{-2}, C_s decreased for only 7% (Supplementary Fig. S5). The ErGO-DLC also has an excellent electrochemical stability; its capacitance keeps unchanged after 10, 000 cycles of charging/discharging even at a high operation current density of 700 μA cm^{-2} (Figure 4b). This result has also been confirmed by comparing the electrochemical impedance spectroscopy (EIS) data of ErGO-DLC before and after testing for 10,000 cycles (Supplementary Fig. S6). On the basis of the above discussion, it is reasonable to conclude that the remarkable electrochemical stability of ErGO[31], 3D interpenetrating microstructure of ErGO electrodes and good contact between ErGO and current collector contribute to the excellent performances of the ErGO-DLC.

The performances of ErGO-DLC can be easily modulated by controlling the time used for the electrodeposition of ErGO layers. When the deposition time increased from 5 to 60 s, the thickness of ErGO

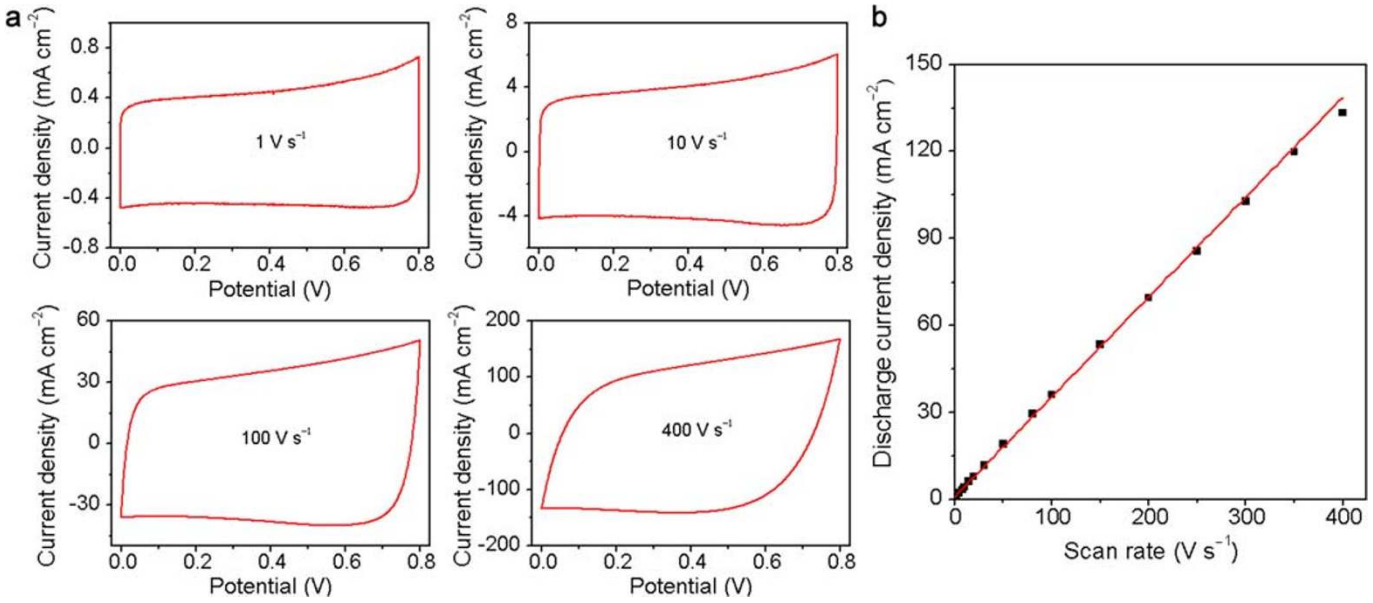

Figure 3 | Cyclic voltammetry (CV) characterizations of ErGO-DLC. (a) CVs obtained at different scan rates in 25% KOH electrolyte. (b) Evolution of the discharge current density versus scan rate.

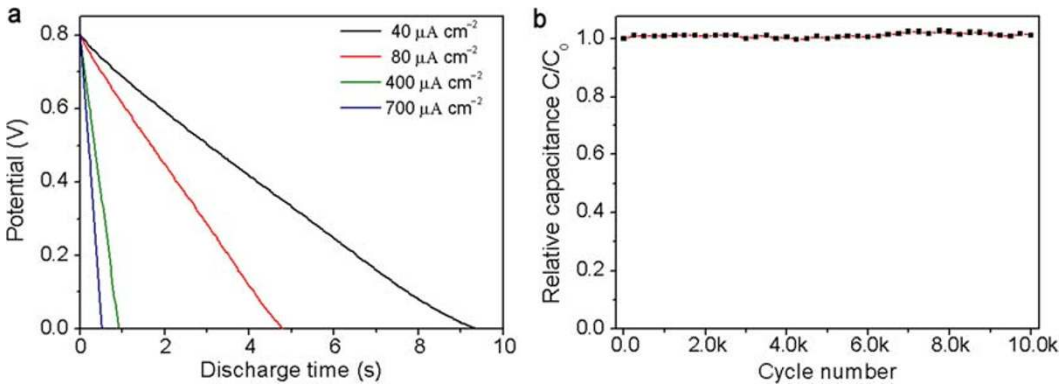

Figure 4 | Galvanostatic charge/discharge characterizations of ErGO-DLC. (a) Discharge curve at a current density of 40, 80, 400 or 700 A cm^{-2}. (b) Lifetime test of ErGO-DLC.

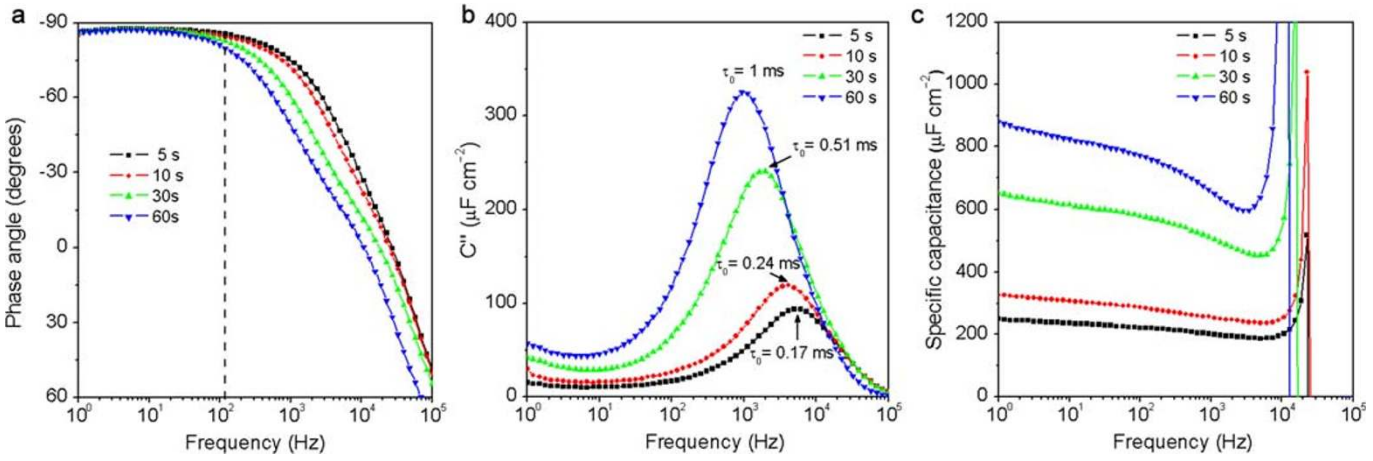

Figure 5 | Comparison of the ErGO-DLCs prepared by electrodepositing ErGO for different time. (a) Plots of impedance phase angle versus frequency. (b) Evolutions of the imaginary parts of the specific capacitances versus frequency. (c) Plots of C_s versus frequency.

layer increased from ~ 10 to ~ 60 μm (Supplementary Fig. S7), which led to an elongation of ionic diffusion paths and a slight increase of ESR (Supplementary Fig. S8). As a result, the phase angle at 120 Hz decreased from −85° to −79.5° (Figure 5a), and τ_0 increased from 170 μs to 1 ms (Figure 5b). Meanwhile, the C_s of the ErGO-DLCs at 1 Hz increased from 250 to 890 μF cm^{-2} (Figure 5c), which can be explained by their thickened ErGO layers.

In summary, we have developed a one-step electrochemical method for preparing ErGO electrodes with 3D interpenetrating microstructures. This method, analogous to electroplating process, is fast, simple, cheap, easy controllable, and readily scalable to industrial levels. The ErGO-DLC shows superior rate-performance. At 120 Hz, it exhibits a phase angle of −84° and RC time constant of 1.35 ms, making it capable of replacing AEC for ac-line filtering. Furthermore, it has a high C_s value of 283 μF cm^{-2} at 120 Hz, which will provide the possibility of greatly reducing the sizes of future electronic circuits.

Methods

GO was prepared by the oxidation of natural graphite powder (325 mesh, Qingdao Huatai Lubricant Sealing S&T Co. Ltd., Qingdao, China) according to a modified Hummers' method reported in the literature (see Supplementary Information for details)[24]. The ErGO electrodes were prepared by electrolyzing 3 mg ml^{-1} graphene oxide (GO) aqueous suspension containing 0.1 M lithium perchlorate ($LiClO_4$) at a potential of −1.2 V for 5–60 s (see Supplementary Information for details). In order to increase the conductivity of ErGO electrodes, they were further reduced in 1 M $LiClO_4$ aqueous solution for another 30 s. Finally, the graphene electrodes were immersed in DI water to remove $LiClO_4$. The treated ErGO electrodes were used to fabricate ErGO-DLC with a symmetrical two-electrode configuration (see Supplementary Information for details).

The ErGO electrodes and GO were freeze-dried and used for further characterization. Raman spectra were recorded on a Renishaw Raman microscope with a 514-nm laser. X-ray photoelectron spectra (XPS) were taken out by using an ESCALAB 250 photoelectron spectrometer (ThermoFisher Scientific, USA). Scanning electron micrographs (SEM) were performed on a field-emission scanning electron microscope (Sirion-200, Japan). All of the electrochemical tests were carried out in a two-electrode system. The electrochemical impedance spectra (EIS) were carried out using a Zahner Ennium electrochemical station (Zahner-Elektrik Gmbh & CoGK, Kronach, Germany) in the frequency range of 1 Hz 100 kHz with a 5 mV ac amplitude. An AEC (1 μF, JAMICON, USA) was used for the comparison with the ErGO-DLC. Cyclic voltammetry and galvanostatic charge/discharge curves were recorded between 0 and 0.8 V using a CHI 760D potentiostat-galvanostat (CH Instruments Inc.).

1. Chmiola, J., Largeot, C., Taberna, P. L., Simon, P. & Gogotsi, Y. Monolithic carbide-derived carbon films for micro-supercapacitors. *Science* **328**, 480–483 (2010).
2. Pech, D. *et al.* Ultrahigh-power micrometre-sized supercapacitors based on onion-like carbon. *Nature Nanotech.* **5**, 651–654 (2010).
3. Simon, P. & Gogotsi, Y. Materials for electrochemical capacitors. *Nature Mater.* **7**, 845–854 (2008).
4. Miller, J. R. & Simon, P. Electrochemical capacitors for energy management. *Science* **321**, 651–652 (2008).
5. Zhang, L. & Zhao, X. Carbon-based materials as supercapacitor electrodes. *Chem. Soc. Rev.* **38**, 2520–2531 (2009).
6. Pandolfo, A. G. & Hollenkamp, A. F. Carbon properties and their role in supercapacitors. *J. Power Sources* **157**, 11–27 (2006).
7. Miller, J. R., Outlaw, R. A. & Holloway, B. C. Graphene double-layer capacitor with ac line-filtering performance. *Science* **329**, 1637–1639 (2010).
8. Niu, C. M., Sichel, E. K., Hoch, R., Moy, D. & Tennent, H. High power electrochemical capacitors based on carbon nanotube electrodes. *Appl. Phys. Lett.* **70**, 1480–1482 (1997).
9. Honda, Y. *et al.* Aligned MWCNT sheet electrodes prepared by transfer methodology providing high-power capacitor performance. *Electrochem. Solid State Lett.* **10**, A106–A110 (2007).
10. Long, J. W., Dunn, B., Rolison, D. R. & White, H. S. Three-dimensional battery architectures. *Chem. Rev.* **104**, 4463–4492 (2004).
11. Rolison, D. R. *et al.* Multifunctional 3D nanoarchitectures for energy storage and conversion. *Chem. Soc. Rev.* **38**, 226–252 (2009).
12. Futaba, D. N. *et al.* Shape-engineerable and highly densely packed single-walled carbon nanotubes and their application as super-capacitor electrodes. *Nature Mater.* **5**, 987–994 (2006).
13. Du, C. & Pan, N. Supercapacitors using carbon nanotubes films by electrophoretic deposition. *J. Power Sources* **160**, 1487–1494 (2006).
14. Zhang, H., Yu, X. & Braun, P. V. Three-dimensional bicontinuous ultrafast-charge and -discharge bulk battery electrodes. *Nature Nanotech.* **6**, 277–281 (2011).
15. Korenblit, Y. *et al.* High-rate electrochemical capacitors based on ordered mesoporous silicon carbide-derived carbon. *ACS Nano* **4**, 1337–1344 (2010).
16. Hou, Y., Cheng, Y., Hobson, T. & Liu, J. Design and synthesis of hierarchical MnO_2 nanospheres/carbon nanotubes/conducting polymer ternary composite for high performance electrochemical electrodes. *Nano Lett.* **10**, 2727–2733 (2010).
17. Lang, X., Hirata, A., Fujita, T. & Chen, M. Nanoporous metal/oxide hybrid electrodes for electrochemical supercapacitors. *Nature Nanotech.* **6**, 232–236 (2011).
18. Zhu, Y. *et al.* Carbon-based supercapacitors produced by activation of graphene. *Science* **332**, 1537–1541 (2011).
19. Yang, X., Zhu, J., Qiu, L. & Li, D. Bioinspired effective prevention of restacking in multilayered graphene films: towards the next generation of high-performance supercapacitors. *Adv. Mater.* **23**, 2833–2838 (2011).
20. Liu, C., Yu, Z., Neff, D., Zhamu, A. & Jang, B. Z. Graphene-based supercapacitor with an ultrahigh energy density. *Nano Lett.* **10**, 4863–4868 (2010).
21. Stoller, M. D., Park, S., Zhu, Y., An, J. & Ruoff, R. S. Graphene-based ultracapacitors. *Nano Lett.* **8**, 3498–3502 (2008).
22. Yoo, J. J. *et al.* Ultrathin planar graphene supercapacitors. *Nano Lett.* **11**, 1423–1427 (2011).
23. Hilder, M., Winther-Jensen, B., Li, D., Forsyth, M. & MacFarlane, D. R. Direct electro-deposition of graphene from aqueous suspensions. *Phys. Chem. Chem. Phys.* **13**, 9187–9193 (2011).
24. Xu, Y., Sheng, K., Li, C. & Shi, G. Self-assembled graphene hydrogel *via* a one-step hydrothermal process. *ACS Nano* **4**, 4324–4330 (2010).
25. Stoller, M. D. & Ruoff, R. S. Best practice methods for determining an electrode material's performance for ultracapacitors. *Energy Environ. Sci.* **3**, 1294–1301 (2010).
26. Gao, W. *et al.* Direct laser writing of micro-supercapacitors on hydrated graphite oxide films. *Nature Nanotech.* **6**, 496–500 (2011).
27. Feng, J. *et al.* Metallic few-layered VS_2 ultrathin nanosheets: high two-dimensional conductivity for in-plane supercapacitors. *J. Am. Chem. Soc.* **133**, 17832–17838 (2011).
28. Qu, D. & Shi, H. Studies of activated carbons used in double-layer capacitors. *J. Power Sources* **74**, 99–107 (1998).
29. Zhang, L. & Shi, G. Preparation of highly conductive graphene hydrogels for fabricating supercapacitors with high rate capability. *J. Phys. Chem. C* **115**, 17206–17212 (2011).
30. Taberna, P. L., Simon, P. & Fauvarque, J. F. Electrochemical characteristics and impedance spectroscopy studies of carbon-carbon supercapacitors. *J. Electrochem. Soc.* **150**, A292–A300 (2003).
31. Toh, H. S., Ambrosi, A., Chua, C. K. & Pumera, M. Graphene oxides exhibit limited cathodic potential window due to their inherent electroactivity. *J. Phys. Chem. C* **115**, 17647–17650 (2011).

Acknowledgements

This work was supported by national basic research program of China (973 Program, 2012CB933402) and natural science foundation of china (51161120361, 91027028). The authors thank Y. Li (Beijing Normal Univ., China) for his help on impendence study.

Author contributions

G. S. and K. S. conceived and designed the experiments. K. S. performed the experiments and analysed the data. Y. S. and W. Y. provided helps in the experiments. K. S., G. S. and C. L. co-wrote the manuscript. All authors discussed the results and commented on the manuscript.

Additional information

Supplementary information accompanies this paper at http://www.nature.com/scientificreports

Competing financial interests: The authors declare no competing financial interests.

How to cite this article: Sheng, K., Sun, Y., Li, C., Yuan, W. & Shi, G. Ultrahigh-rate supercapacitors based on eletrochemically reduced graphene oxide for ac line-filtering. *Sci. Rep.* 2, 247; DOI:10.1038/srep00247 (2012).